Comparative Studies on *in Vitro* Methods for Evaluating *in Vivo* Function of MDR1 P-Glycoprotein

Yasuhisa Adachi,[1] Hiroshi Suzuki,[1] and Yuichi Sugiyama[1,2]

Received June 8, 2001; accepted August 21, 2001

Purpose. MDR1 P-glycoprotein (P-gp) plays an important role in determining drug disposition. The purpose of the present study was to establish *in vitro* models to predict the *in vivo* function of P-gp.
Methods. As an *in vitro* method, the transcellular transport of 12 compounds across the monolayer of Caco-2- and MDR1-transfected cells was examined. The ability of these compounds to stimulate the ATP hydrolysis was also determined using the isolated membrane fraction expressing P-gp. As a parameter to describe the *in vivo* P-gp function, we calculated the brain-to-plasma concentration ratio of compounds in mdr1a/1b knockout mice divided by the same ratio in wild type mice.
Results. A good correlation was observed between the *in vitro* flux ratio across the monolayer and *in vivo* P-gp function for 12 compounds. Although all compounds that stimulated ATP hydrolysis were significantly transported by P-gp, some compounds were transported by P-gp without significantly affecting ATP hydrolysis.
Conclusion. Collectively, the *in vitro* flux ratio across monolayers of P-gp-expressing cells may be used to predict *in vivo* P-gp function. The extent of ATP-hydrolysis *in vitro* may also be a useful parameter for *in vivo* prediction, particularly for eliminating P-gp substrates in high-throughput screening procedures.

KEY WORDS: MDR1 P-glycoprotein; blood–brain barrier; transcellular transport; ATP-hydrolysis; mdr1 knockout mice.

INTRODUCTION

MDR1 P-glycoprotein (P-gp) initially was cloned from tumor cell lines that acquired multidrug resistance as an ATP-dependent transporter responsible for the cellular extrusion of a series of antitumor drugs (1,2). It is now well established that P-gp is also expressed in many normal tissues, including the intestinal epithelium, hepatocytes, renal tubular cells, and brain capillary endothelial cells, and plays an important role in drug disposition (3–5). This fact has been investigated in detail by comparing the drug disposition between normal mice and their mdr1 knockout counterparts (4–6). The oral absorption, along with the brain penetration, of P-gp substrates was significantly lower in normal mice compared with mdr1a (–/–) mice (6). Recently, it was also demonstrated that, in humans, a single nucleotide polymorphism in MDR1 gene results in a significantly higher bioavailability of orally administered digoxin as a result of the decreased expression level of P-gp (7). In addition, simultaneous administration of P-gp modulators enhances the intestinal absorption and brain penetration of P-gp substrates in both experimental animals and humans (8–11). To discover the extent of the interaction between drugs and P-gp *in vivo* is obviously of great importance when developing novel drugs and establishing safe and efficient drug therapeutic schedules (12,13). The quantitative prediction of penetration of P-gp substrates across the blood–brain barrier is particularly important because the penetration of a drug into the brain is directly related to its toxicity in the central nervous system. For example, mdr1a (–/–) mice are much more sensitive to the toxic central nervous system effects of ivermectin compared with wild-type mice (14,15).

Recently, several types of *in vitro* models have been proposed to determine the substrate specificity of P-gp. In the present study, we quantitatively examined the function of P-gp in *in vitro* models and compared the results with those obtained in *in vivo*. In the *in vitro* models, we determined the transcellular transport of 12 compounds across monolayers of Caco-2 cells that endogenously express human MDR1 and human MDR1 cDNA-transfected LLC-PK1 cells. We also determined the ability of these 12 compounds to stimulate ATP hydrolysis using the isolated plasma membrane from High Five cells expressing P-gp. These *in vitro* parameters were compared with the *in vivo* function of P-gp located on the cerebral endothelial cells, which was determined as the value of the brain-to-plasma concentration ratio of respective compounds in mdr1a (–/–) mice divided by the same ratio in normal mice.

MATERIALS AND METHODS

Materials

[^{3}H]Daunomycin (185 GBq/mmol), [^{3}H]digoxin (703 GBq/mmol), [^{3}H]diazepam (3052 GBq/mmol), [^{3}H]dexamethasone (1500 GBq/mmol), [^{3}H]17β estradiol-17β-D-glucuronide ($E_2$17βG; 1628 GBq/mmol), [^{3}H]progesterone (5291 GBq/mmol), and [^{3}H]verapamil (3145 GBq/mmol) were purchased from New England Nuclear (Boston, MA). [^{3}H]Cimetidine (574 GBq/mmol), [^{3}H]cyclosporin A (259 GBq/mmol), and [^{3}H]vinblastine (411 GBq/mmol) were purchased from Amersham (Buckinghamshire, UK). [^{3}H]Quinidine (740 GBq/mmol) was purchased from ARC (St. Louis, MO). Unlabeled loperamide was purchased from Sigma (St. Louis, MO).

Transcellular Transport Studies across Cultured Cell Monolayers

LLC-PK1- and MDR1-transfected LLC-PK1 (LLC-MDR1) cells, donated by Dr. P. Borst (The Netherlands Cancer Institute, Amsterdam, The Netherlands), were grown under conditions described previously (16,17). Briefly, LLC-PK1 and LLC-MDR1 were grown in M199 medium (Sigma) supplemented with 10% fetal bovine serum and 100 U/mL penicillin G and streptomycin sulfate and incubated at 37°C in 5% CO_2. Caco-2 cells were grown in Dulbecco's modified eagle medium (high glucose) supplemented with 10% fetal bovine serum, 2 mM L-glutamine, 100 U/mL penicillin G, and streptomycin sulfate and 1% nonessential amino acids and incubated at 37°C in 5% CO_2. LLC-PK1 and LLC-MDR1 cells were seeded at a density of 1.4×10^5 cells/well on

[1] Graduate School of Pharmaceutical Sciences, The University of Tokyo Hongo, Bunkyo-ku, Tokyo 113-0033, Japan.
[2] To whom correspondence should be addressed. (e-mail: sugiyama@mol.f.u-tokyo.ac.jp)

0724-8741/01/1200-1660/0

porous polyethylene terephthalate membrane filters (3 μm pore size, 0.31 cm^2 filter area, Falcon® culture insert, Becton Dickinson, Franklin Lakes, NJ). Caco-2 cells were seeded at a density of 3×10^4 cells/well on the same polyethylene terephthalate membrane filters. Cells were cultured in 24-well plates and were used for the transport studies 4 days after seeding for LLC-PK1 and LLC-MDR1 and after 21–23 days for Caco-2 cells (18,19). For transcellular transport experiments, each cell monolayer was washed with phosphate-buffered saline before pre-incubation for 1 h in OPTI-MEM® (Gibco BRL, Rockville, MD) for LLC-PK1 and LLC-MDR1 cells and in Hank's balanced salt solution for Caco-2 cells. Transcellular transport experiments were initiated by adding the solution of test compounds to the apical (250 μL) or basal (950 μL) side. The concentrations of compounds were as follows: [^{3}H]cimetidine (37 kBq/mL, 64.5 nM), [^{3}H]cyclosporin A (9.25 kBq/mL, 35.7 nM), [^{3}H]daunomycin (37 kBq/mL, 200 nM), [^{3}H]digoxin (37 kBq/mL, 52.6 nM), [^{3}H]diazepam (37 kBq/mL, 12.1 nM), [^{3}H]dexamethasone (37 kBq/mL, 24.7 nM), [^{3}H]$E_2$17βG (37 kBq/mL, 22.7 nM), [^{3}H]progesterone (37 kBq/mL, 7 nM), [^{3}H]quinidine (37 kBq/mL, 50 nM), [^{3}H]verapamil (37 kBq/mL, 11.8 nM), [^{3}H]vinblastine (9.25 kBq/mL, 22.5 nM), and unlabeled loperamide (1 μM). At 1, 2, and 4 h for LLC-PK1 and LLC-MDR1 cells and at 1 and 2 h for Caco-2 cells, aliquots of medium in the receiver side were taken to determine the transported amount of each compound.

For the previously described isotopically labeled compounds, the transported amount was determined by measuring their radioactivity in a liquid scintillation counter (model 1900 TR, Packard, Meriden, CT). For loperamide, quantification was performed by high-performance liquid chromatography (HPLC) connected to a tandem mass spectrometer analytical system (MS/MS, model TSQ7000, Thermo-Quest, San Jose, CA) after extraction using a solid phase extraction column (OASIS® HLB, Waters, Milford, MA). As internal standards, haloperidol was used for loperamide quantification. HPLC analysis was performed in an Inertsil® ODS 3 (5 μm, 4.6 &mult; 150 mm) (GL Sciences, Tokyo, Japan). The mobile phase was 55% distilled water containing 0.1% acetic acid and 45% methanol. The flow rate of mobile phase was 0.5 mL/min. Then, the eluent of HPLC was ionized using the electrosplay interface. Full-scan MS/MS spectra were obtained, and the following transition was monitored: 477.2–265.7 for loperamide and 376.0–164.4 for haloperidol.

The permeability-surface area (PS) product across the monolayer was defined as follows:

$$\text{PS product} = A/t/Co \tag{1}$$

where t, A, and Co represent the incubation time, the transported amount of compounds per mg protein of cell monolayer, and the initial concentration of compounds in the donor side, respectively. Flux ratio across the monolayer was defined as

$$\text{flux ratio} = \frac{PS_{b\ to\ a}}{PS_{a\ to\ b}} \tag{2}$$

where $PS_{b\ to\ a}$ and $PS_{a\ to\ b}$ represent the PS product in the basal-to-apical direction and the apical-to-basal direction, respectively. In LLC-PK1/LLC-MDR1 cells, the corrected flux ratio was defined by Equation 3:

$$\text{corrected flux ratio} = \frac{\text{flux ratio in LLC} - \text{MDR1 cells}}{\text{flux ratio in LLC} - \text{PK1 cells}} \tag{3}$$

Stimulation of ATP Hydrolysis

The ability of compounds to stimulate ATP hydrolysis was examined using the membrane fraction from High Five (BTI-TN5B1-4) cells expressing P-gp, which was purchased from Gentest (Boston, MA) (20,21). The membrane fraction from High Five cells (667 μg protein/mL) was incubated in 60 μL medium consisting of 50 mM 2-morpholinoethanesulfonic acid, 50 mM KCl, 2 mM dithiothreitol, 2 mM ethyleneglycol bis(2-aminoethyl ether)-tetraacetic acid, 2 mM Tris HCl, and 5 mM NaN_3 (pH 7.4) with or without test compounds. After pre-incubation for 5 min at 37 °C, experiments were initiated by the addition of 20 μL of Mg ATP solution. The final ATP concentration in the medium was 4 mM. The reaction was terminated at 20 min by the addition of 30 μL of 10% sodium dodecyl sulfate. To this reaction mixture, 180 μL of solution containing 1.3% sulfuric acid, 0.2% ammonium molybdate, 2.3% trichloroacetic acid, and 1% ascorbic acid was added to quantify the released amount of inorganic phosphate in a plate reader (model 3550, Bio–Rad, Hercules, CA) at a wavelength of 655 nm. The vanadate-sensitive ATP hydrolysis was determined by subtracting the value obtained with the vanadate co-incubated membrane fraction from vanadate-free membrane fraction.

Determination of Tissue Distribution of Compounds in Normal and Mdr1a/b (–/–) Mice

Experiments were performed on male mdr1a/1b (–/–) mice (bodyweight 23–28 g, Taconic Farms Inc., NY) and FVB-inbred mice (bodyweight 23–28 g, Taconic Farms Inc., NY) as the normal mice. *In vivo* drug disposition studies were performed as described previously (19,22) in male mice (7–10 weeks of age). The radiolabeled compounds {[^{3}H]daunomycin (2 kBq (177 pmol)/g body weight), [^{3}H]progesterone (2 kBq (351 pmol)/g body weight and [^{3}H]diazepam (3 kBq (318 pmol)/g body weight)}, dissolved in saline solution (5 μL/g body weight), were injected over a 5-s period into the tail vein of mice lightly anesthetized with diethyl ether. After 30 min, the animals were anesthetized and completely exsanguinated by cardiac puncture. Heparinized plasma was obtained from the collected blood by centrifugation. Harvested tissues (brain, liver, and kidney) were weighed and homogenized with saline. The radioactivity was determined in a liquid scintillation counter (model 1900 TR, Packard) after addition of 10 mL of Hionic Fluor® (Packard) to the aliquots of plasma (50 μL) and homogenate (200 μL) specimens. The amount of unmetabolized compounds was quantified by HPLC (model VP-5, Shimadzu, Kyoto, Japan) equipped with a fluorescence detector for daunomycin and by thin-layer chromatography for diazepam and progesterone. The tissue-to-plasma concentration ratio was calculated from the concentrations of the unmetabolized compounds. Daunomycin quantification was performed under gradient condition using an Inertsil® C8 (5 μm) 4.6 × 150-mm column (GL Sciences, Tokyo, Japan). The mobile phase was 10 mM ammonium phosphate and acetonitrile. Gradient condition was as follows: from 25% acetonitrile at time zero to 40% acetonitrile at 20 min with the

flow rate of 1 mL/min. The eluent was collected every minute to determine the radioactivity. The thin-layer chromatography analysis of diazepam was performed according to the method described previously (23) on Merck 5714 silica gel plate (5 × 20 cm) (Merck, Darmsdadt, Germany), with the solvent system consisted of hexane:chloroform:ethanol:acetic acid = 10:10:1:1. For progesterone, Merck 5714 silica gel plate (5 × 20 cm) (Merck) was used for the analysis with the solvent system consisted of cyclohexane: ethyl acetate = 2:1. Radioactivity associated with the non-metabolized compounds was determined in a liquid scintillation counter (model 1900 TR, Packard) after scraping the gel of the plate.

As a parameter to describe the *in vivo* function of P-gp located on the cerebral endothelial cells, the Kp_{brain} ratio was defined as follows:

$$Kp_{brain}\ \text{ratio} = \frac{\text{the brain - to - plasma concentration ratio in mdr1(–/–)mice}}{\text{the brain - to - plasma concentration ratio in normal mice}} \quad (4)$$

For the other seven compounds, the Kp_{brain} ratios were taken from the reported data (9,14,16,17,19,24). Results are given as the mean ± standard error unless otherwise denoted.

RESULTS

Transcellular Transport across Cultured Cell Monolayers

Figure 1 shows the time profiles for the transcellular transport of 12 compounds in Caco-2 cells. The calculated PS products, along with the flux ratio in Caco-2 cells, are summarized in Table I. In the same manner, time profiles for the transcellular transport of the 12 compounds across LLC-PK1 and LLC-MDR1 monolayers are shown in Figure 2. The results, along with the corrected flux ratio, are also summarized in Table II. As reported previously, for good substrates for P-gp (such as quinidine and digoxin), the basal-to-apical flux markedly exceeded to that in the opposite direction (Figs. 1 and 2). In contrast, for poor substrates for P-gp (such as progesterone and $E_2$17βG), the extent of the flux was almost the same in the two directions (Figs. 1 and 2). The substrate specificity determined in the present study (Figs. 1 and 2) is consistent with previous observations (16,17). The rank order of the flux ratio of compounds was very similar in both LLC-MDR1 and Caco-2 cells (Figs. 1 and 2).

To quantitatively compare the transport activity mediated by P-gp between Caco-2 and LLC-MDR1 monolayers, the correlation of the flux ratio between the two cell lines was examined (Fig. 3). Figure 3 clearly demonstrates the significant positive correlation in the flux ratio and/or corrected flux ratio between Caco-2 and LLC-PK1/LLC-MDR1. It can also be seen that the absolute values of the flux ratio is higher in LLC-MDR1 cells than that in Caco-2 cells (Fig. 3a), which may be accounted for by assuming a higher expression level of P-gp in LLC-MDR1.

Stimulation of ATP Hydrolysis

In another *in vitro* experiment, we examined the stimulatory effect of the 12 compounds on ATP-hydrolysis in a

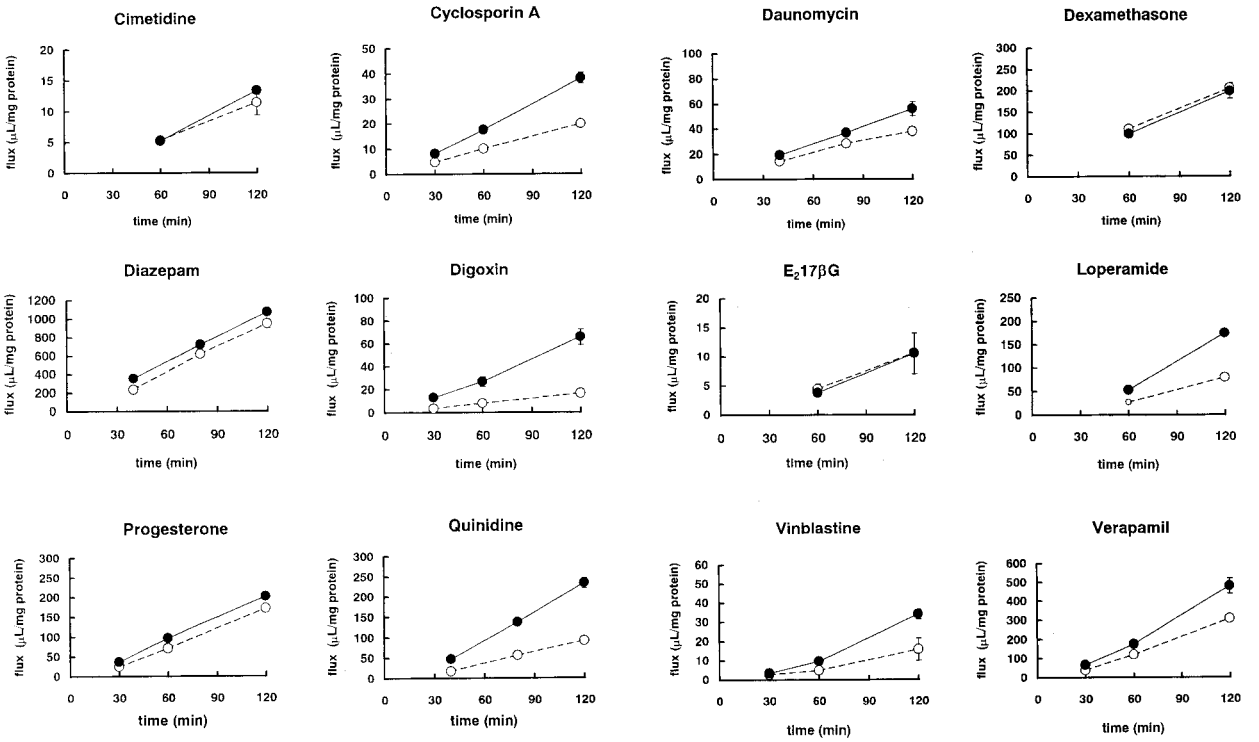

Fig. 1. Time profiles for the transcellular transport of 12 compounds across Caco-2 monolayers. Transcellular transport of 12 compounds across Caco-2 monolayers was determined as a function of time. The ligand concentrations used in these experiments are described in the text. The ordinate represents the volume of distribution (μL/mg protein), which was obtained by the amount of ligands transferred to the acceptor side divided by the initial concentration of ligands on the donor side. Each point and vertical bar represents the mean ± standard error of three independent experiments. ○, apical-to-basal flux; ●, basal-to-apical flux.

Table I. Kinetic Parameters for Penetration across Caco-2 Monolayers

Test compounds	$PS_{a\ to\ b}$ (μL/min/mg protein)	$PS_{b\ to\ a}$ (μL/min/mg protein)	Flux ratio
Cimetidine	0.0953 ± 0.0099	0.112 ± 0.003	1.17 ± 0.13
Cyclosporine A	0.166 ± 0.001	0.319 ± 0.010	1.92 ± 0.06
Daunomycin	0.316 ± 0.004	0.467 ± 0.027	1.48 ± 0.09
Dexamethasone	1.71 ± 0.13	1.66 ± 0.03	0.968 ± 0.076
Diazepam	7.90 ± 0.16	8.81 ± 0.18	1.11 ± 0.03
Digoxin	0.138 ± 0.007	0.549 ± 0.033	3.98 ± 0.31
$E_2$17βG	0.0883 ± 0.002	0.0875 ± 0.017	0.991 ± 0.193
Loperamide	0.654 ± 0.035	1.45 ± 0.03	2.21 ± 0.13
Progesterone	1.43 ± 0.10	1.68 ± 0.12	1.18 ± 0.12
Quinidine	0.760 ± 0.025	1.95 ± 0.06	2.56 ± 0.12
Verapamil	2.56 ± 0.07	3.99 ± 0.19	1.56 ± 0.09
Vinblastine	0.132 ± 0.028	0.283 ± 0.012	2.15 ± 0.46

Based on the results shown in Figure 1, the PS products and flux ratio across Caco-2 monolayer were calculated according to Equations 2 and 7, respectively. The results are shown as the mean ± standard error. The standard error was calculated according to the law of propagation of error.

P-gp-expressing membrane fraction as a function of the medium concentration of the test compounds. In the absence of test compounds, the ATPase activities associated with the P-gp-expressing membrane fractions were 3–6 nmol of Pi/min/mg protein, which is consistent with the previous observations (21). A potent stimulatory effect was exhibited by cyclosporin A and quinidine (Fig. 4). However, some ligands with stimulatory effect on P-gp mediated ATP hydrolysis rather inhibited the ATPase activity at higher concentrations (Fig. 4). In contrast, only a minimal effect was exhibited by digoxin and loperamide (Fig. 4), irrespective of the fact that these two compounds were significantly transported by P-gp across the cultured cell monolayers (Figs. 1 and 2). Kinetic parameters determined by analysis are summarized in Table III.

Tissue Distribution of Compounds in Normal and Mdr1a/b (–/–) Mice

For daunomycin, progesterone, and diazepam, the tissue distribution in normal and mdr1a/b (–/–) mice was quantitatively determined. For daunomycin, the brain-to-plasma concentration ratio in mdr1a/1b (–/–) mice (1.63 ± 0.08) was significantly higher ($P < 0.05$) than that in normal mice (0.91 ± 0.01). This *in vivo* finding is consistent with the *in vitro* transport studies, which indicate that daunomycin is vectorially transported across cultured cell monolayers (Figs. 1 and 2). In contrast, no significant difference was observed in the tissue-to-plasma concentration ratio for other peripheral tissues such as liver and kidney (data not shown).

In contrast to daunomycin, no significant difference was observed for progesterone and diazepam in the brain-to-plasma concentration ratio between normal mice (1.45 ± 0.12 and 3.35 ± 0.11, respectively) and mdr1a/b (–/–) mice (1.34 ±

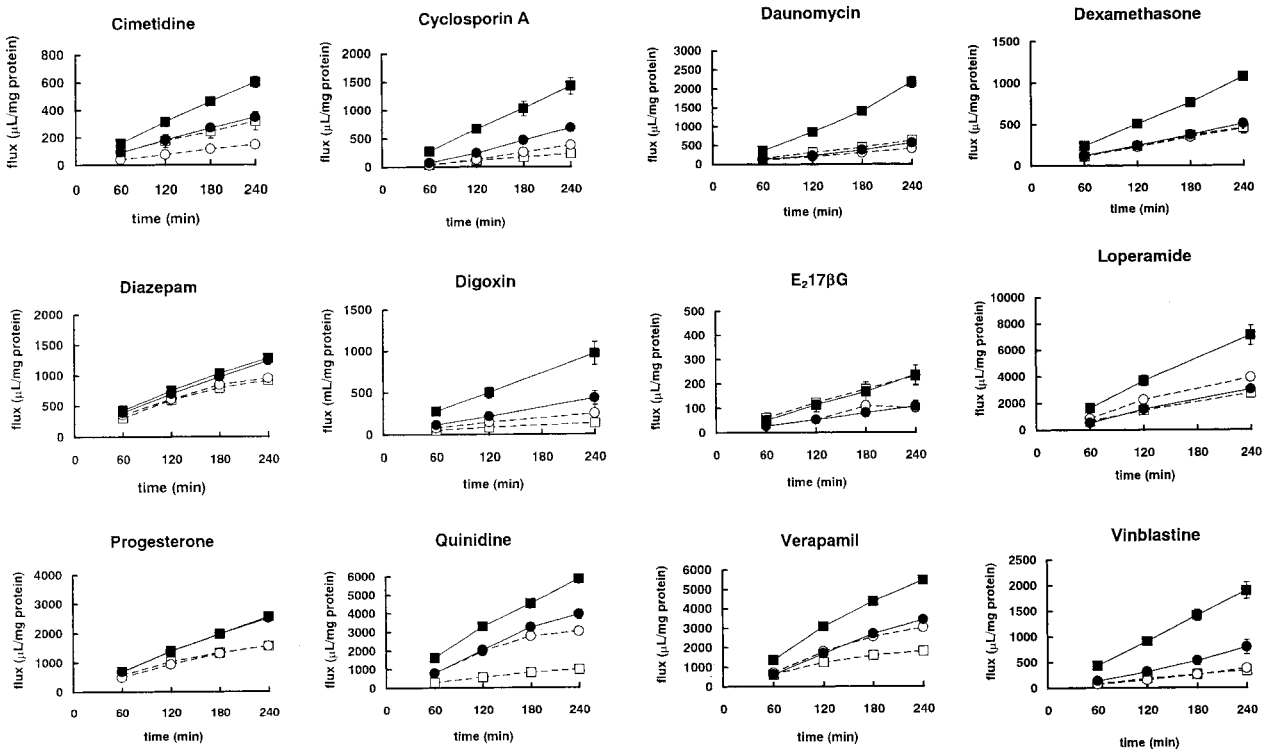

Fig. 2. Time profiles for the transcellular transport of 12 compounds across LLC-PK1 monolayers. Transcellular transport of 12 compounds across LLC-PK1 and LLC-MDR1 monolayers was determined as a function of time. The ligand concentrations used in these experiments are described in the text. The ordinate represents the volume of distribution (μL/mg protein), which was obtained from the amount of ligands transferred to the acceptor side divided by the initial concentration of ligands on the donor side. Each point and vertical bar represents the mean ± standard error of three independent experiments. ○, apical-to-basal flux across LLC-PK1; ●, basal-to-apical flux across LLC-PK1; □, apical-to-basal flux across LLC-MDR1; ■, basal-to-apical flux across LLC-MDR1.

Table II. Kinetic Parameters for the Penetration across LLC-PK1 Monolayers

	LLC-PK1			LLC-MDR1			
Test compounds	$PS_{a\ to\ b}$ (μL/min/mg protein)	$PS_{b\ to\ a}$ (μL/min/mg protein)	Flux ratio	$PS_{a\ to\ b}$ (μL/min/mg protein)	$PS_{b\ to\ a}$ (μL/min/mg protein)	Flux ratio	Corrected flux ratio
Cimetidine	0.620 ± 0.110	1.44 ± 0.12	2.34 ± 0.46	1.32 ± 0.28	2.51 ± 0.16	1.90 ± 0.42	0.810 ± 0.237
Cyclosporine A	1.59 ± 0.12	2.87 ± 0.25	1.81 ± 0.21	0.98 ± 0.07	5.94 ± 0.62	6.09 ± 0.78	3.37 ± 0.59
Daunomycin	1.75 ± 0.04	2.35 ± 0.03	1.34 ± 0.03	2.64 ± 0.27	9.08 ± 0.61	3.45 ± 0.42	2.57 ± 0.32
Dexamethasone	1.85 ± 0.05	2.12 ± 0.14	1.15 ± 0.09	1.89 ± 0.19	4.49 ± 0.16	2.38 ± 0.25	2.08 ± 0.28
Diazepam	3.94 ± 0.26	5.15 ± 0.01	1.31 ± 0.09	3.78 ± 0.03	5.32 ± 0.09	1.41 ± 0.03	1.08 ± 0.08
Digoxin	1.03 ± 0.21	1.80 ± 0.21	1.74 ± 0.40	0.560 ± 0.058	4.03 ± 0.33	7.29 ± 0.94	4.20 ± 1.11
$E_2$17βG	0.410 ± 0.023	0.440 ± 0.092	1.07 ± 0.23	0.960 ± 0.162	0.980 ± 0.17	1.02 ± 0.25	0.950 ± 0.306
Loperamide	16.4 ± 0.4	12.7 ± 0.9	0.78 ± 0.06	11.3 ± 0.1	29.7 ± 3.1	2.62 ± 0.27	3.38 ± 0.43
Progesterone	6.44 ± 0.36	10.5 ± 0.1	1.62 ± 0.09	6.48 ± 0.21	10.7 ± 0.3	1.64 ± 0.08	1.01 ± 0.08
Quinidine	12.6 ± 0.8	16.4 ± 1.1	1.30 ± 0.12	4.07 ± 0.03	24.4 ± 1.0	5.99 ± 0.26	4.59 ± 0.46
Verapamil	12.5 ± 0.1	14.2 ± 0.3	1.14 ± 0.03	7.51 ± 0.14	22.7 ± 0.7	3.02 ± 0.11	2.66 ± 0.12
Vinblastine	1.56 ± 0.09	3.30 ± 0.33	2.12 ± 0.25	1.39 ± 0.01	7.88 ± 0.68	5.65 ± 0.48	2.66 ± 0.39

Based on the results shown in Figure 2, PS products, flux ratio, and corrected flux ratio across LLC-PK1/LLC-MDR1 were calculated according to Equations 2, 7, and 8, respectively. The results are shown as the mean ± standard error. The standard error was calculated according to the law of propagation of error.

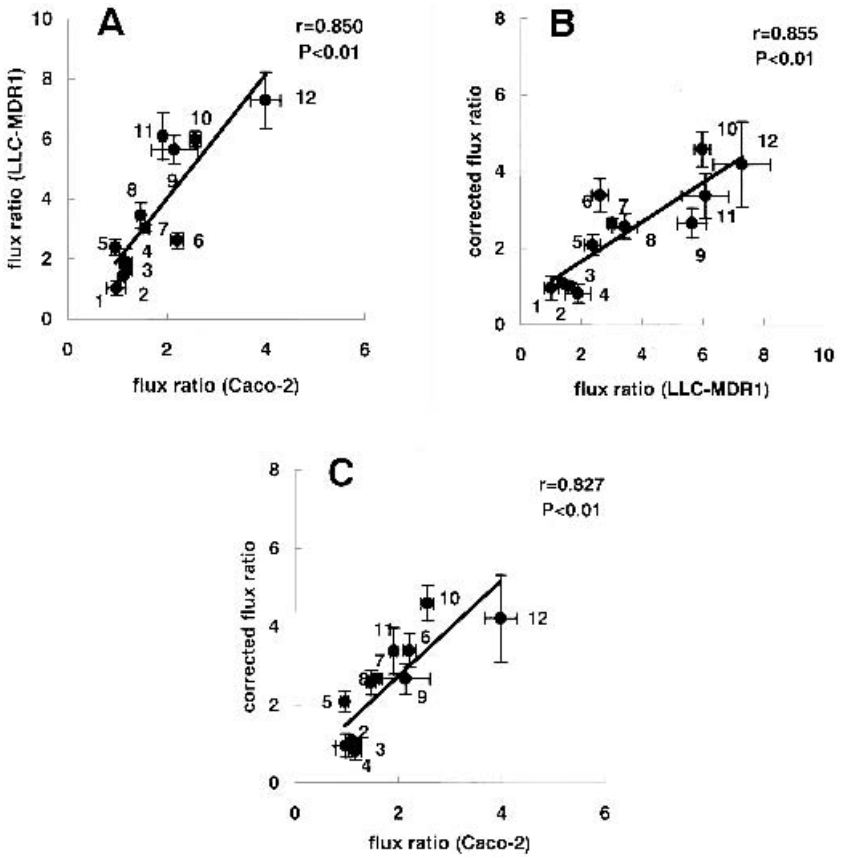

Fig. 3. Correlation of the flux between Caco-2 and LLC-PK1 monolayers. Based on the results shown in Figures 1 and 2, the correlation of the flux between Caco-2 and LLC-PK1 monolayers was examined. A, Correlation between the flux ratio in Caco-2 and that in LLC-MDR1. B, Correlation between the flux ratio and the corrected flux ratio in LLC-PK1 and LLC-MDR1. C, Correlation between the flux ratio in Caco-2 and the corrected flux ratio in LLC-PK1/LLC-MDR1. Each point and vertical bar represents the mean ± standard error, which was calculated according to the law of propagation of error. 1, $E_2$17βG; 2, diazepam; 3, progesterone; 4, cimetidine; 5, dexamethasone; 6, loperamide; 7, verapamil; 8, daunomycin; 9, vinblastine; 10, quinidine; 11, cyclosporin A; 12, digoxin.

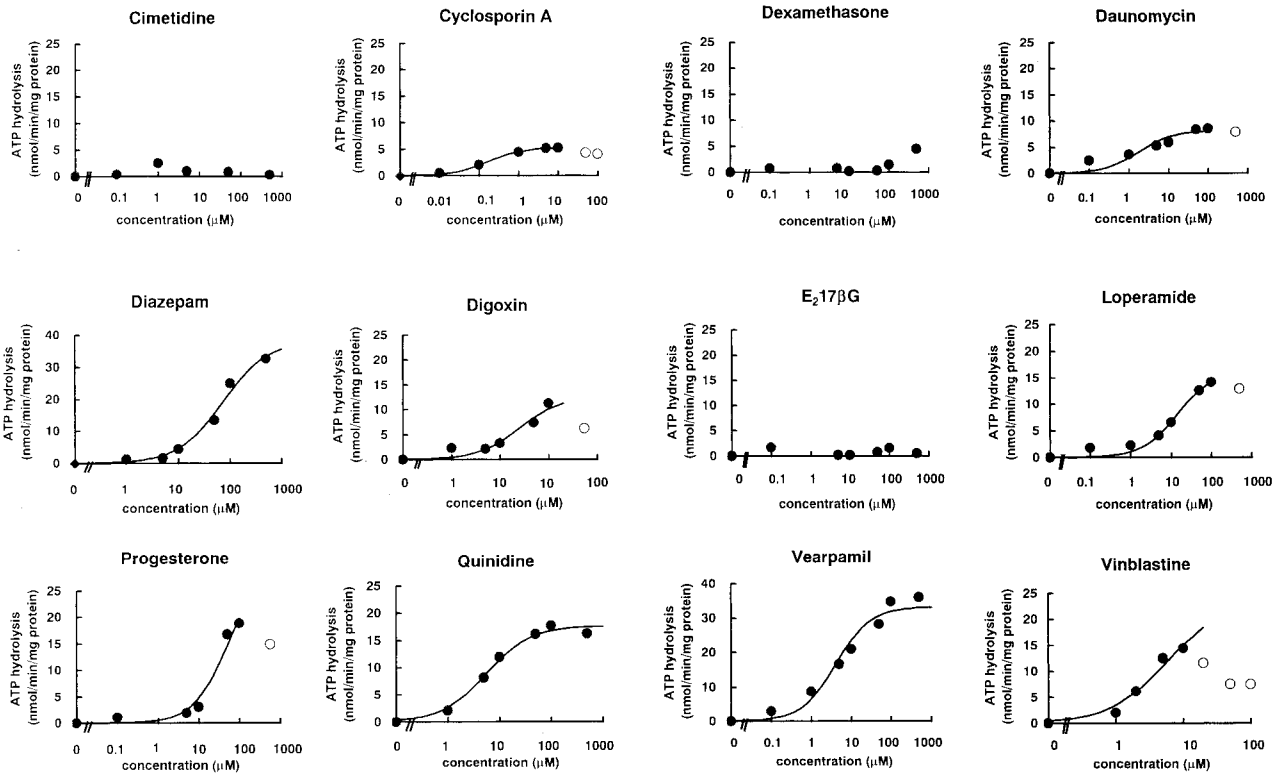

Fig. 4. Effect of 12 compounds on ATP-hydrolysis by P-gp. Concentration-dependent effect of 12 compounds on the ATP hydrolysis in the membrane fraction from High Five cells expressing P-gp was determined as a function of the medium concentration. The membrane fraction (40 μg protein / 60 μL medium) was incubated for 20 min at 37°C to determine the amount of inorganic phosphate released from 4 mM ATP. The data were fitted to the Michaelis–Menten equation to determine the estimated concentration for half-maximum activation and the maximum activation. Solid line represents the fitted line and the closed symbols represent the data used for the analysis. Data with the open symbols were not used for the analysis. Each point represents the mean of two independent experiments.

0.18 and 3.24 ± 0.03, respectively), which is consistent with the *in vitro* findings with cultured cell monolayers (Figs. 1 and 2).

Correlation between *in Vitro* and *in Vivo* Results

The correlation between the previously described *in vivo* and *in vitro* experimental results was examined to assess the suitability of *in vitro* methods for quantitatively predicting *in vivo* disposition. There was a significant positive correlation between the *in vitro* flux ratio across Caco-2 and LLC-MDR1 monolayers and the *in vivo* Kp_{brain} ratio (Fig. 5, A and B; $r = 0.812$, $P < 0.01$ and $r = 0.869$, $P < 0.01$, respectively). A higher correlation coefficient was observed between the corrected flux ratio across LLC-PK1/LLC-MDR1 cells and the *in vivo* Kp_{brain} ratio (Fig. 5C; $r = 0.892$, $P < 0.01$). Although all compounds that stimulated ATP hydrolysis were significantly transported by P-gp both *in vitro* and *in vivo,* some compounds (such as dexamethasone) were transported by P-gp without significantly affecting the ATP hydrolysis (Fig. 5D).

DISCUSSION

In the present study, comparative studies were performed both *in vitro* and *in vivo* to identify the most reliable *in vitro* method to predict the *in vivo* P-gp function. We used the Kp_{brain} ratio as a parameter to describe the P-gp function on cerebral endothelial cells. By normalizing the brain-to-plasma concentration ratio in mdr1 knockout mice by the same ratio in normal mice, we can cancel out the effect of the degree of plasma protein binding, binding to brain, and possible involvement of transporters other than P-gp and, therefore, simply estimate the function of P-gp. As shown in Figure 5, *in vivo* P-gp function can be quantitatively predicted by using the corrected flux ratio and, to a lesser extent, by using the flux ratio, across the cultured cell monolayers.

The suitability of these *in vitro* methods should be discussed in relation to a number of theoretical considerations. According to the pharmacokinetic model shown in Scheme 1, $PS_{a\ to\ b}$ and $PS_{b\ to\ a}$ across LLC-PK1 cells monolayer are given by

$$Ps_{a\ to\ b} = PS_{a,inf} \times \frac{PS_{b,eff}}{PS_{a,eff} + PS_{b,eff}} \quad (5)$$

$$PS_{b\ to\ a} = PS_{b,inf} \times \frac{PS_{a,eff}}{PS_{a,eff} + PS_{b,eff}} \quad (6)$$

where $PS_{a,inf}$ and $PS_{a,eff}$ represent the PS product for the influx and efflux across the apical membrane, and $PS_{b,inf}$ and $PS_{b,eff}$ represent the PS product for the influx and efflux across the basal membrane, respectively (Scheme 1). In addition, $PS_{p\text{-}gp}$ represents the PS product mediated by P-gp (Scheme 1). Consequently, the flux ratio across Caco-2 and LLC-MDR1 monolayers, originally defined by Equation 2, is given by:

$$\text{flux ratio} = \frac{PS_{b,inf} \times (PS_{a,eff} + PS_{p-gp})}{PS_{a,inf} \times PS_{b,eff}} \quad (7)$$

Table III. Kinetic Parameters for ATP Hydrolysis

	K_m (μM)	V_{max} (nmol Pi/min/mg protein)	V_{max}/K_m (mL/min/mg protein)
Cyclosporin A	0.170 ± 0.020	5.29 ± 0.09	31.1 ± 3.7
Daunomycin	1.74 ± 1.08	8.17 ± 0.92	4.70 ± 2.96
Diazepam	72.4 ± 16.5	38.2 ± 2.9	0.527 ± 0.127
Digoxin	25.9 ± 18.1	12.7 ± 4.0	0.490 ± 0.375
Loperamide	13.8 ± 4.4	16.0 ± 1.5	1.16 ± 0.38
Progesterone	53.6 ± 30.7	30.4 ± 7.8	0.568 ± 0.357
Quinidine	5.42 ± 0.95	17.6 ± 0.6	3.24 ± 0.58
Verapamil	4.06 ± 1.38	33.2 ± 3.0	8.18 ± 2.87
Vinblastine	5.71 ± 3.20	23.7 ± 6.5	4.15 ± 2.59
Cimetidine	Silent	Silent	—
Dexamethasone	Silent	Silent	—
$E_2$17βG	Silent	Silent	—

Data shown in Figure 4 were analyzed according to the Michaelis–Menten equation to determine the apparent V_{max} and K_m values. The results are shown as the mean ± computer-calculated standard error. "Silent" refers to a substrate that does not alter the P-gp-mediated ATP-hydrolysis.

The corrected flux ratio across LLC-PK1/LLC-MDR1, originally defined by Equation 3, therefore, is given by

$$\text{corrected flux ratio} = 1 + \frac{PS_{p\text{-}gp}}{PS_{a,eff}} \quad (8)$$

In the same manner, the PS product for the unidirectional influx across the blood–brain barrier from blood into brain and that for the opposite direction is given by

$$PS_{blood\text{-}to\text{-}brain} = PS_{l,inf} \times \frac{PS_{al,eff}}{PS_{l,eff} + PS_{al,eff}} \quad (9)$$

$$PS_{brain\text{-}to\text{-}blood} = PS_{al,inf} \times \frac{PS_{l,eff}}{PS_{l,eff} + PS_{al,eff}} \quad (10)$$

where $PS_{l,inf}$ and $PS_{l,eff}$ represent the PS product for the influx and efflux across the luminal membrane, and $PS_{al,inf}$ and $PS_{al,eff}$ represent the PS product for the influx and efflux across the antiluminal membrane of the cerebral endothelial

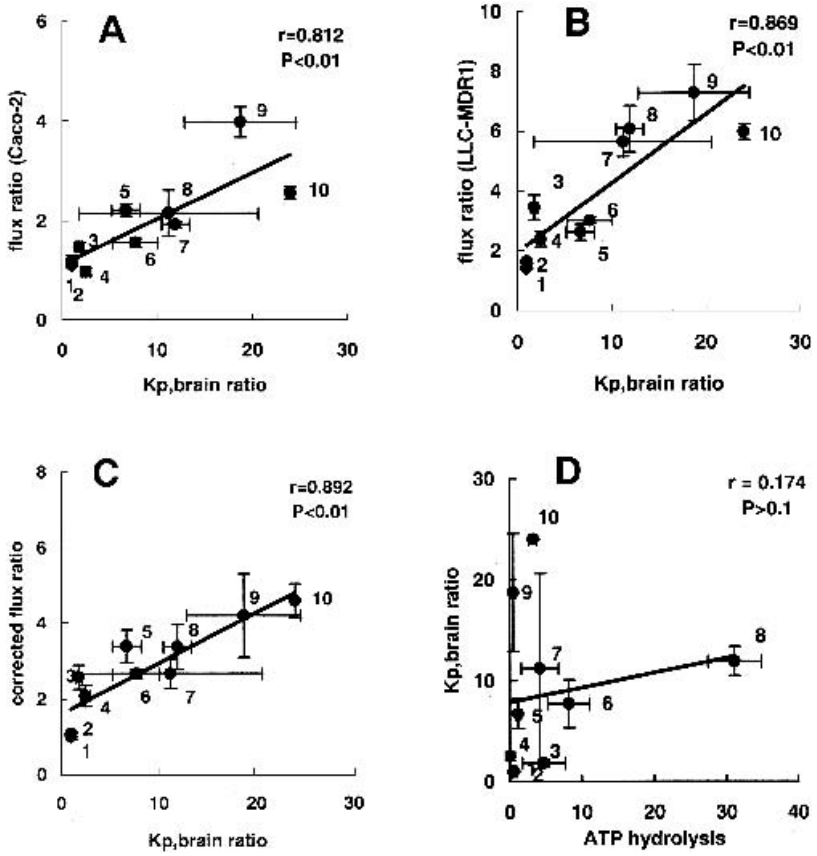

Fig. 5. Correlation of P-gp function determined in *in vitro* transcellular transport studies, ATP hydrolysis studies and *in vivo* brain penetration studies. Data listed in Tables I, II, and III were summarized to examine the correlation between *in vivo* and *in vitro* P-gp function. Previously reported data for the Kp_{brain} ratio of 7 compounds were also included; the reference to this source is given in the text. A, Correlation between Kp_{brain} ratio and flux ratio in Caco-2 cells. B, Correlation between Kp_{brain} ratio and flux ratio in LLC-MDR1 cells. C, Correlation between Kp_{brain} ratio and corrected flux ratio in LLC-PK1/LLC-MDR1 cells. D, Correlation between Kp_{brain} ratio and stimulatory effect on the ATP hydrolysis (V_{max}/K_m). Each point and vertical bar represents the mean ± standard error, which was calculated according to the law of propagation of error. 1, diazepam; 2, progesterone; 3,daunomycin; 4, dexamethasone; 5, loperamide; 6, verapamil; 7, vinblastine; 8, cyclosporin A; 9, digoxin; 10, quinidine.

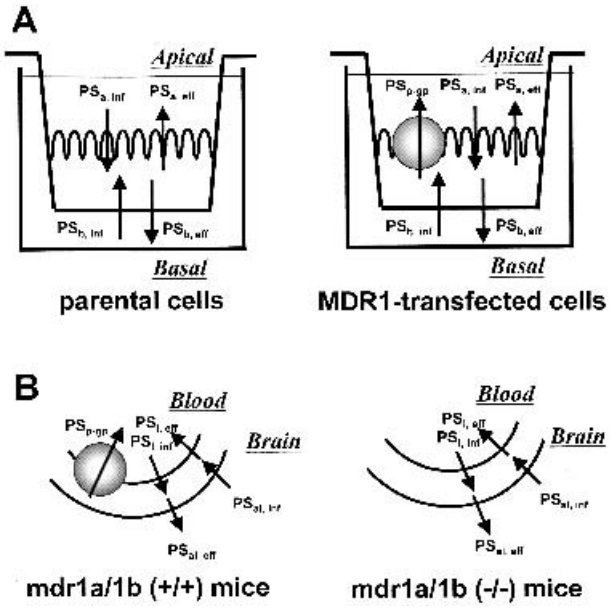

Scheme 1. Schematic diagram illustrating the PS products for the penetration of ligands across the plasma membrane. A and B represent the PS products across the cultured cell monolayers and those across the cerebral endothelial cells. $PS_{a,inf}$ and $PS_{a,eff}$ represent the PS products for the influx and efflux across the apical membrane, respectively. $PS_{b,inf}$ and $PS_{b,eff}$ represent the PS products for the influx and efflux across the basal membrane, respectively. $PS_{p\text{-}gp}$ represents the PS product for P-gp mediated efflux across the apical membrane; $PS_{l,inf}$ and $PS_{l,eff}$ represent the PS products for the influx and efflux across the luminal membrane of cerebral endothelial cells, respectively. $PS_{al,inf}$ and $PS_{al,eff}$ represent the PS products for the influx and efflux across the antiluminal membrane of cerebral endothelial cells, respectively. $PS_{p\text{-}gp}$ represents the PS product for the P-gp-mediated efflux across the luminal membrane.

cells, respectively (Scheme 1). Because the Kp_{brain} is given by $PS_{blood\text{-}to\text{-}brain}$ / $PS_{brain\text{-}to\text{-}blood}$, Kp_{brain} is given by

$$Kp_{brain} = \frac{PS_{l,inf} \times PS_{al,eff}}{PS_{al,inf} \times PS_{l,eff}} \quad (11)$$

By taking the ratio of Kp_{brain} in mdr1a/b (–/–) to that in normal mice, the ratio in Kp_{brain} is given by

$$Kp_{brain}\ \text{ratio} = 1 + \frac{PS_{p\text{-}gp}}{PS_{l,eff}} \quad (12)$$

Considering Equations 8 and 12, it is to be expected that, if we plot the corrected flux ratio across LLC-PK1/LLC-MDR1 cells and the Kp_{brain} ratio between mdr1a/b (–/–) and normal mice, a straight line should be obtained that passes through the coordinates (1,1). Indeed, such a clear correlation was obtained experimentally (Fig. 5C). A good correlation between these *in vitro* and *in vivo* parameters (Fig. 5C) suggests that, at least for the compounds used in the present study, there are minimal species differences in the substrate recognition by P-gp between mice and humans. The difference in the absolute value of the slope of the line from unity (Fig. 5C) may result from the difference in the expression level of mdr1a in the cerebral endothelial cells compared with that of MDR1 in LLC-MDR1 cells and/or the difference in the intrinsic activity between mdr1a and MDR1.

Such correlation of P-gp function between *in vitro* and *in vivo* parameters was also reported independently by Yamazaki *et al.* (25) after submission of the present article. A good correlation was reported between the *in vitro* Kp_{brain} ratio and the flux ratio across LLC-PK1 cells transfected with cDNA for mouse mdr1a (25). For some compounds, however, the species difference was observed in substrate transport between human and mouse P-gp, and consequently, the correlation coefficient was significantly lower if the Kp_{brain} ratio in mice was compared with the flux ratio across the monolayer transfected with human MDR1 cDNA (25).

We should also consider the reason why there is a good correlation between the flux ratio across the cultured cell monolayers and the *in vivo* Kp_{brain} ratio (Fig. 5, A and B). If transporters other than P-gp are not involved in the ligand transport, the flux ratio across the cultured cell monolayers, given by Equation 7, can be reduced to Equation 8 and, therefore, it is reasonable to expect a linear correlation between the flux ratio across the *in vitro* cell monolayers and the *in vivo* Kp_{brain} ratio. A slight, but significant reduction in the correlation coefficients between the flux ratio and the Kp_{brain} ratio compared with that between the corrected flux ratio and the Kp_{brain} ratio (Fig. 5, A–C) may be accounted for by considering the involvement of other transport mechanism(s) for several types of compounds.

In the present study, we also compared the magnitude of the stimulatory effect on ATP hydrolysis and the Kp_{brain} ratio (Fig. 5D). It was found that several compounds (such as verapamil and vinblastine) inhibited the ATPase activity at higher concentrations (Fig. 4), which is consistent with the previous observations (26,27). At the present time, we do not have an explanation to account for these results. However, it has been hypothesized that, at higher concentrations, these compounds may interfere with the membrane lipid and/or may interact with a low-affinity inhibitory site (28,29). To analyze the effect of compounds able to stimulate the ATPase activity, we calculated the apparent V_{max} and K_m values based on the Michaelis–Menten equation after subtraction of the ATPase activity in the absence of compounds (Table III). The apparent K_m values determined in the present study (Table III) were similar to those reported previously, e.g., for daunomycin, progesterone, and verapamil, the observed and reported values were 1.74 μM (Table III) vs. 2 μM (20), 53.6 μM (Table III) vs. 30 μM (29) and 4.06 μM (Table III) vs. 2 μM (29), respectively. Differences were observed for vinblastine because the apparent K_m value determined in the present study (5.71 μM; Table III) was significantly higher than the previously reported value (0.8 μM; Reference 29). Moreover, we found that some compounds (such as dexamethasone) are transported via P-gp without significantly affecting the ATPase activity (Figs. 1, 2, and 4). Such phenomena have also been reported previously; it has been reported that PSC833, substrates for P-gp, did not stimulate the ATPase activity (26). Consequently, we were unable to obtain any significant correlation between the magnitude of stimulatory effect of compounds, defined as V_{max}/K_m, and transport activity mediated by P-gp (Fig. 5D). A much more detailed molecular biologic mechanism-linking ligand transport and ATP hydrolysis is required (30,31). However, because ATP hydrolysis was observed for all P-gp substrates (Fig. 4), this *in vitro* model may be useful, particularly for eliminating P-gp substrates in the high-throughput screening procedures.

In conclusion, it was demonstrated that the *in vivo* P-gp

function, given as the Kp_{brain} ratio between mdr1a/b (–/–) and normal mice, can be quantitatively predicted by the corrected flux ratio across LLC-PK1/LLC-MDR1 monolayers and, to a lesser extent, by the flux ratio across Caco-2 and LLC-MDR1 monolayers. These *in vitro* models may be useful for quantitatively predicting the *in vivo* brain penetration of MDR1 substrates. Moreover, the excellent predictability of *in vivo* P-gp function from *in vitro* monolayer models was further supported by theoretical considerations. A significant correlation was not obtained between *in vivo* P-gp function and the *in vitro* stimulatory effect on ATP-hydrolysis and some exceptions were observed between ligand transport and ATP-hydrolysis. A more detailed understanding of the molecular mechanism for the association of ligand transport and ATP-hydrolysis by P-gp is required to solve this problem.

ACKNOWLEGMENTS

This work was supported by Grant-in-Aid from the Ministry of Health, Labor and Welfare.

REFERENCES

1. C. J. Chen, J. E. Chin, K. Ueda, D. P. Clark, I. Pastan, M. M. Gottesman, and I. B. Roninson. Internal duplication and homology with bacterial transport proteins in the mdr1 (P-glycoprotein) gene from multidrug-resistant human cells. *Cell* **47**:381–389 (1986).
2. K. Ueda, D. P. Clark, C. J. Chen, I. B. Roninson, M. M. Gottesman, and I. Pastan. The human multidrug resistance (mdr1) gene. cDNA cloning and transcription. *J. Biol. Chem.* **262**:505–508 (1987).
3. S. V. Ambudkar, S. Dey, C. A. Hrycyna, M. Ramachandra, I. Pastan, and M. M. Gottesman. Biochemical, cellular, and pharmacological aspects of the multidrug transporter. *Annu. Rev. Pharmacol. Toxicol.* **39**:361–398 (1999).
4. V. J. Wacher, J. A. Silverman, Y. Zhang, and L. Z. Benet. Role of P-glycoprotein and cytochrome P450 3A in limiting oral absorption of peptides and peptidomimetics. *J. Pharm. Sci.* **87**:1322–1330 (1998).
5. L. Z. Benet, T. Izumi, Y. Zhang, J. A. Silverman, and V. J. Wacher. Intestinal MDR transport proteins and P450 enzymes as barriers to oral drug delivery. *J. Control. Release* **62**:25–31 (1999).
6. A. H. Schinkel. Pharmacological insights from P-glycoprotein knockout mice. *Clin. Pharmacol. Ther.* **36**:9–13 (1998).
7. S. Hoffmeyer, O. Burk, O. von Richter, H. P. Arnold, J. Brockmöller, A. Johne, I. Cascorbi, T. Gerloff, I. Roots, M. Eichelbaum, and U. Brinkmann. Functional polymorphisms of the human multidrug-resistance gene: Multiple sequence variations and correlation of one allele with P-glycoprotein expression and activity *in vivo*. *Proc. Natl. Acad. Sci. USA* **97**:3473–3478 (2000).
8. U. Mayer, E. Wagenaar, B. Dorobek, J. H. Beijnen, P. Borst, and A. H. Schinkel. Full blockade of intestinal P-glycoprotein and extensive inhibition of blood–brain barrier P-glycoprotein by oral treatment of mice with PSC833. *J. Clin. Invest.* **100**:2430–2436 (1997).
9. H. Kusuhara, H. Suzuki, T. Terasaki, A. Kakee, M. Lemaire, and Y. Sugiyama. P-glycoprotein mediates the efflux of quinidine across the blood–brain barrier. *J. Pharmacol. Exp. Ther.* **283**:574–580 (1997).
10. D. J. Edwards, M. E. Fitzsimmons, E. G. Schuetz, K. Yasuda, M. P. Ducharme, L. H. Warbasse, P. M. Woster, J. D. Schuetz, and P. Watkins. 6′,7′-Dihydroxybergamottin in grapefruit juice and Seville orange juice: Effects on cyclosporine disposition, enterocyte CYP3A4, and P-glycoprotein. *Clin. Pharmacol. Ther.* **65**: 237–244 (1999).
11. H. Suzuki and Y. Sugiyama. Role of metabolic enzymes and efflux transporters in the absorption of drugs from the small intestine. *Eur. J. Pharm. Sci.* **12**:3–12 (2000).
12. D. K. Yu. The contribution of P-glycoprotein to pharmacokinetic drug–drug interactions. *J. Clin. Pharmacol.* **39**:1203–1211 (1999).
13. M. Verschraagen, C. H. W. Koks, J. H. M. Schellens, and J. H. Beijnen. P-glycoprotein system as a determinant of drug interactions: The case of digoxin-verapamil. *Pharmacol. Res.* **40**:301–306 (1999).
14. A. H. Schinkel, J. J. M. Smit, O. van Tellingen, J. H. Beijnen, E. Wagenaar, L. van Deemter, C. A. A. M. Mol, M. A. van der Valk, E. C. Robanus-Maandag, H. P. J. te Riele, A. J. M. Berns, and P. Borst. Disruption of the mouse moder1a P-glycoprotein gene leads to a deficiency in the blood-brain barrier and to increased sensitivity to drugs. *Cell* **77**:491–502 (1994).
15. G. Y. Kwei, R. F. Alvaro, Q. Chen, H. J. Jenkins, C. E. A. C. Hop, C. A. Keohane, V. T. Ly, J. R. Strauss, R. W. Wang, Z. Wang, T. R. Pippert, and D. R. Umbenhauer. Disposition of ivermectin and cyclosporin A in CF-1 mice deficient in mdr1a P-glycoprotein. *Drug Metab. Dispos.* **27**:581–587 (1999).
16. A. H. Schinkel, E. Wagenaar, L. van Deemter, C. A. A. M. Mol, and P. Borst. Absence for the mdr1a P-glycoprotein in mice affects tissue distribution and pharmacokinetics of dexamethasone, digoxin, and cyclosporin A. *J. Clin. Invest.* **96**:1698–1705 (1995).
17. A. H. Schinkel, E. Wagenaar, C. A. A. M. Mol, and L. van Deemter. P-glycoprotein in the blood-brain barrier of mice influences the brain penetration and pharmacological activity of many drugs. *J. Clin. Invest.* **97**:2517–2524 (1996).
18. A. Tsuji, H. Takanaga, I. Tamai, and T. Terasaki. Transcellular transport of benzoic acid across Caco-2 cells by a pH-dependent and carrier-mediated transport mechanism. *Pharm. Res.* **11**:30–37 (1994).
19. R. B. Kim, M. F. Fromm, C. Wandel, B. Leake, A. J. J. Wood, D. M. Roden, and G. R. Wilkinson. The drug transporter P-glycoprotein limits oral absorption and brain entry of HIV-1 protease inhibitors. *J. Clin. Invest.* **101**:289–294 (1998).
20. B. Sarkadi, E. M. Price, R. C. Boucher, U. A. Germann, and G. A. Scarborough. Expression of the human multidrug resistance cDNA in insect cells generates a high activity Drug-stimulated membrane ATPase. *J. Biol. Chem.* **267**:4854–4858 (1992).
21. F. J. Sharom, Xiaohong Yu, Peihua Lu, Ronghua Liu, J. W. K Chu, K. Szabo, M. Muller, C. D. Hose, A. Monks, A. Varadi, J. Seprodi, and B. Sarkadi. Interaction of the P-glycoprotein Multidrug transporter (MDR1) with high affinity peptide chemosensitizers in isolated membranes, reconstituted system and intact cells. *Biochem. Pharmacol.* **58**:571–586 (1999).
22. J. W. Jonker, E. Wagenaar, L. van Deemter, R. Gottschlich, H. M. Bender, J. Dasenbrock, and A. H. Schinkel. Role of blood–brain barrier P-glycoprotein in limiting brain accumulation and sedative side-effects of asimadoline, a peripherally acting analgaesic drug. *Br. J. Pharmacol.* **127**:43–50 (1999).
23. C. F. Neville, S. Ninomiya, N. Shimada, T. Kamataki, S. Imaoka, and Y. Funae. Characterization of specific cytochrome P450 enzyme responsible for the metabolism of diazepam hepatic microsomes of adult male rats. *Biochem. Pharmacol.* **45**:59–65 (1993).
24. N. H. Hendrikse, A. H. Schinkel, E. G. E. De Vries, E. Fluks, W. T. A. Van der Graaf, A. T. M. Willemsen, W. Vaalburg, and E. J. F. Franssen. Complete *in vivo* reversal of P-glycoprotein pump function in the blood-drain barrier visualized with positron emission tomography. *Br. J. Pharmacol.* **124**:1413–1418 (1998).
25. M. Yamazaki, W. E. Neway, T. Ohe, I. Chen, J. F. Rowe, J. H. Hochman, M. Chiba, and J. H. Lin. *In vitro* substrate identification studies for P-glycoprotein-mediated transport: species difference and predictability of *in vivo* results. *J. Pharmacol. Exp. Ther.* **296**:723–735 (2001).
26. T. Litman, T. Zeuthen, T. Skovsgaard, and W. D. Stein. Structure-activity relationships of P-glycoprotein interacting drugs: kinetic characterization of their effects on ATPase activity. *Biochim. Biophys. Acta* **1361**:159–168 (1997).
27. E. Buxbaum. Co-operative binding sites for transported substrates in the multiple drug resistance transporter Mdr1. *Eur. J. Biochem.* **265**:64–70 (1999).
28. S. Drori, G. D. Eytan, and Y. G. Assaraf. Potentiation of anticancer-drug cytotoxicity by multidrug-resistance chemosensitizers involves alterations in membrane fluidity leading to increased membrane permeability. *Eur. J. Biochem.* **228**:1020–1029 (1995).
29. M. J. Borgnia, G. D. Eytan, and Y. G. Assaraf. Competition of hydrophobic peptides, cytotoxic drugs, and chemosensitizers on a common P-glycoprotein pharmacophore as revealed by Its ATPase activity. *J. Biol. Chem.* **271**:3163–3171 (1996).
30. K. Ueda, A. Yoshida, and T. Amachi. Recent progress in P-glycoprotein research. *Anti-Cancer Drug Design* **14**:115–121 (1999).
31. Z. E. Sauna and S. V. Ambudkar. Evidence for a requirement for ATP hydrolysis at two distinct steps during a single turnover of the catalytic cycle of human P-glycoprotein. *Proc. Natl. Acad. Sci. USA* **97**:2515–2520 (2000).